The biological effect of 2.45 GHz microwaves on the viability and permeability of bacterial and yeast cells

Evans K. Ahortor,[1] Dmitry Malyshev,[1] Catrin F. Williams,[2] Heungjae Choi,[2] Jonathan Lees,[2] Adrian Porch,[2] Les Baillie[1]

[1]School of Pharmacy and Pharmaceutical Science, Cardiff University, Redwood Building, King Edward VII Avenue, Cardiff, CF10 3NB, Wales, United Kingdom

[2]School of Engineering, Cardiff University, Queen's Buildings, Newport Road, Cardiff, CF24 3AA Wales, United Kingdom

Corresponding author: ahortorek@cardiff.ac.uk/evansahortorkwame@gmail.com

Abstract

Microwaves are a form of non-ionising radiation composed of electric (E) and magnetic (H) fields and are absorbed by biological tissues with a high water content. Our study investigated the effect of the E field, H field and a combination of both (E+H) fields exposure of structurally diverse micro-organisms, at a frequency of 2.45 GHz. We observed that the exposure to a microwave E field of amplitude 9.3 kV/m had no significant effect on cell viability; however, it did increase membrane permeability of *M. smegmatis* to propidium iodide and to a range of different sized dextran particles in *E. coli, S. aureus, C. albicans* and *M. smegmatis.* The permeability of propidium iodide was observed in microwave treated cell (*M. smegmatis*) but not in heat-treated cells. Permeability of 3 kDa sized fluorescently labelled dextrans was observed across all cells types; however, this was found not to be the case for larger 70 kDa

dextran particles. In terms of efflux, DNA was detected following E field exposure of *M. smegmatis.* In contrast, H field exposure had no effect on cell viability and did not contribute to increase cells membrane to dextran particles. In conclusion, this study shows that microwave generated E fields can temporarily disrupt membrane integrity without detrimentally impacting on cell viability. This approach has the potential to be developed as a high efficiency electropermeabilisation method and as a means of releasing host DNA to support diagnostic applications.

Introduction

Microwaves (MWs) are a form of non-ionising radiation, with numerous applications in the health, food and communications industries (1,2). As a portion of the electromagnetic spectrum, they are composed of alternating electric (E) and magnetic (H) fields and can be absorbed by different materials including biological tissues (3). One of the most widely used frequency bands for Industrial, Scientific, and Medical (ISM) applications is from 2.4 to 2.5 GHz in MW heating ('thermal') and excitation ('non-thermal'). Within most aqueous materials, including biological tissues, MWs at a frequency of around 2.45 GHz penetrate to a depth of a few cm. The exponential decay of MW field strength into such materials is a result of the absorption of MW energy via the direct interaction of the E and H field with the material. Small samples, such as individual cells and bacteria, are fully penetrated by the MW H fields. While the effects of MWs on biological structures have been widely reported, their precise mode of action remains elusive (4,5).

The mechanism of MW action is primarily attributed to the generation of heat (thermal effects), while the contribution, if any, of non-thermal effects have yet to be established (6). Membrane disruption can be induced by the E or H fields (7,8). Biological membranes, contain electrically

excitable molecules (e.g. proteins and lipids) which change their behaviour in the presence of an E field (9,10). In the case of membrane phospholipids, when voltage drop associated with the applied E field is greater than the membrane potential, the lipids reorient to the E field, resulting in membrane destabilisation and the formation of transient gaps (pores) (11,12). The effective transmembrane potential required to induce membrane poration is between 0.2-1.0 V (13,14). The size and duration of these pores are modulated by MW parameters such as frequency, pulse length, amplitude and duration of MW exposure (15). For instance, longer pulse duration forms larger pores and vice versa. Typically, about 10-12 kV/cm is required to electroporate cells of *E. coli* and *S. thermophilus* but can differ for other cell types such as yeast and mycobacteria (8,16).

For the past 50 years, studies on the biological effect of MWs have increased tremendously owing to their potential detriment to humans. Their effect on neurons, hormones, brain tissues, enzyme kinetics, ion channels, reproductive organs and immune cells are known (17) while studies of 2.45 GHz on bacterial cells under nonthermal conditions are scarce. In a recent study, it was found that 2.45 GHz MWs could alter the membranes of *E. coli* cells (18). Considering the significant differences that exist in cell membranes belonging to different taxonomic groups, there could be varying interaction with different cells following MW exposure. In another study, membrane permeability was observed in range of structurally different micro-organisms but at a frequency of 18 GHz (19–21). The separate effect of 2.45 GHz MWs (E, H and E+H) is of research interest as the mechanism of MW action remains an enigma. The ability of MWs to enhance influx of foreign materials (e.g. DNA, drugs) across membranes is well known, but the associated loss of cell viability has a detrimental effect on the efficiency of this approach (13). In light of the knowledge gap and the challenge in membrane disruption/ electroporation, we aimed at identifying a process which maximises membrane

permeabilization while minimising loss of cells viability. We explored the potential of low amplitude E and H MW fields at 2.45 GHz MW to permeabilize a structurally diverse range of micro-organisms by measuring the uptake of propidium iodide (PI) varying sized dextran particles (3, 10 and 70 kDa) and the release of nucleic acid.

Materials and Methods

Bacterial and yeast cells, culture and preparation

The following bacterial and yeast strains were used in this study: *Escherichia coli* (NCTC 1093), *Staphylococcus aureus* (NCTC 13373) and *Mycobacterium smegmatis* (NCTC 8159) were cultured in Luria-Bertani (LB) broth (Oxoid). *Candida albicans* (NCPF 3179) was cultivated in yeast extract, Low-Dusting (LD) (BD, Difco). Cells were harvested and resuspended in sterile distilled water to a concentration of 1×10^8 CFU/mL, corresponding to an optical density of 0.8 measured at a wavelength of 600 nm with a UV/Vis spectrophotometer (Ultrospec 2100 pro, Biochrom, USA).

Single-mode cavity as MW applicator

MW cavities have been widely used as sensors and applicators (22–24). Empty cavity resonators create electromagnetic standing waves within their space when excited by an external E or H field, producing resonant peak at the swept frequency domain. E and H field distribution inside the cavity can be perturbed by introducing small volume of sample, resulting in the change of resonant frequency and bandwidth which can be related to the dielectric properties of the sample under test. In single-mode cavities this relationship is mathematically well defined so the dielectric properties can be easily extracted by measuring the change in resonant parameters (22). Also, the high sensitivity of the single-mode cavity leads to more intense field in the area of interest for a given power input when used as an applicator (24). In

addition to that, the locations of E and H field maxima can be separated in single-mode cavities. This allows us to investigate the effect of E, E and H, and H field on biological cells and tissues.

MW system components

Our TM_{010} cavity is designed to investigate the effect of 2.45 GHz MWs on biological structures. 2.45 GHz was chosen because it is the frequency used in ISM applications. An aluminium cylindrical cavity resonator designed at 2.45 GHz (internal radius = 46 mm, internal height = 40 mm) is used as a MW applicator. The cavity was critically coupled with a loop-terminated N-type connector, which couples to the MW H field around the cavity's inner circumference. To minimize an undesired heating, the design of the system using a switch and directional coupler 1 allows MW to be delivered in pulses. The MW system is designed to use a low power signal generator (1mW) which is then amplified to a maximum of 30W, while the power delivered to the cavity was limited to 12 W (41 dBm) in our experiment.

Synchronized signal generation, switching on/off, and data acquisition from three power sensors are controlled by LabVIEW user interface. The combination of switch, attenuator, and the directional coupler 1 produce microwave pulse with high on/off isolation (>50 dB) without turning on and off MW signal generator. This also minimizes unwanted heating at the pulse OFF state due to leakage power. Power sensors 2 and 3 monitor the incident and the reflected power respectively. Power sensor 1 also monitors the reflected power, which is technically redundant but was included as a safety measure in case the low-cost power sensors 2 and 3 fail. As shown in the schematic diagram in Fig 1, the bench-top MW application system used in this study consists of the following elements: a MW signal generator (TEG-4000-1, Telemakus), a MW switch (TES-7000-50, Telemakus), 20 dB directional couplers 1 and 2 (ZABDC20-322H-S+, Mini-Circuits), MW power amplifier (ZHL-30W-252-S+), MW circulator (NG-3548,

Racal-MESL), MW power sensor 1 (ZRP-Z51, Rhode & Schwarz), and power sensors 2 and 3 (TED-8000-40, Telemakus).

When excited in its TM_{010} mode, the cavity produces distinct E and H fields with the maximal E field obtained axially while maximal H field is obtained just inside the circumference, as shown in Fig. 2. Each sample contained in a 0.2 mL mini-micro tube (Alpha laboratories, UK) was inserted into the cavity, one at a time, to allow samples to be exposed to the E (position A), H (position C) and E+H fields (position B), respectively. The peak E and H field intensities in the cavity at the central and circumferential sample positions within the TM_{010} mode are calculated to be approximately 9.3 kV/m and 70 A/m (corresponding to a magnetic flux density of 87.9 μT), respectively. By placing the sample tube into the three-hole TM_{010} mode cavity, the field is perturbed (22,25,26). For this reason, the Q value (representing the amount power dissipated into the sample) at the three sample positions was measured using sample volumes of 170 μL (Table I). Based on our calculations, indeed, the power dissipated into the sample, which is proportional to the E field is halved at the E+H positions and totally diminished at the H field position.

MW irradiation

Determination of cell viability in MW treated samples

The viability of cells (*S. aureus*, *E. coli*, *C. albicans* and *M. smegmatis*) was determined after exposures to MW E, H and E+H fields. MW power was pulsed at 1 % duty cycle for 60 sec. The pulse period and the ON time were kept constant at 1000 ms and 10 ms, respectively. Sample excitation was performed at room temperature and repeated 5 more times with a 2 min interval between each excitation cycle. Cell viability was determined immediately after MW exposure using the drop count method (27). Cells were incubated overnight at 37 ºC and the dilution containing countable bacterial colonies (between 30 and 300 were used to determine

viability. *M. smegmatis*, *E. coli* and *S. aureus* were plated on LB agar and *C. albicans* was plated on yeast extract agar. Cells without MW treatment were included as negative controls.

Quantification of DNA released following MW treatment

Using similar MW exposure conditions, sample volume and concentration, 170 µL aliquots of test micro-organism (*M. smegmatis*) in a 0.2 mL mini-micro tube (Alpha laboratories, UK) were placed in the different radial positions of the TM_{010} mode resonant cavity to determine the effect of exposure to E, H and E+H fields on DNA release. DNA concentration of the bacterial suspension was determined immediately following exposure to E, H and E+H fields using the Qubit dsDNA BR Assay Kit (Invitrogen) and Qubit 3.0 fluorometer (Invitrogen). Suspensions of MW treated cells (20 µL) were mixed with 180 µL of dsDNA BR Qubit assay reagent and vortexed. The concentration of dsDNA was then quantified using the Qubit 3.0 fluorometer (Invitrogen). Untreated bacterial suspension was used as a negative control.

MW induced membrane disruption

To determine the effect of MW (E, H and E+H) field exposure on cell wall permeability, first the entry of PI into *M. smegmatis* was determined. Next, the entry of a range of fluorescently labelled dextran particles into micro-organisms of structural diversity was then examined.

Permeability to propidium iodide (PI)

One millilitre suspension of *M. smegmatis* (1 mL, 10^8 cfu/mL) were stained with 1 µL PI solution (1 mg/mL, Sigma Aldrich) for 10 min at room temperature. PI stained cells (170 µL) were treated with MW (E, E+H, H) fields using the above conditions or heat treated in a water bath at 37 °C for 10 min. Fluorescent intensity was quantified in microplate reader (Tecan® Infinite 200 PRO). PI was excited (535 nm) and the emission was collected at 617 nm. PI

stained cells without Fluorescent stained cells without MW or heat treatment were included as controls.

Permeability to dextran particles

Suspensions of the following size particles were prepared in water and tested; 3 kDa (Cat. No. D3308) and 70 kDa (Cat. No. D1818) both tetramethylrhodamine (TMR) and 10 kDa Alexa 488 (Cat. No. D22910), all purchased from Fisher Scientific, UK. Cells were treated with MW pulsed at 1% duty cycle for 60 sec at RT in the MW cavity. Sample excitation was repeated 5 more times with a 2 min interval between each irradiation cycle to minimise sample heating. MW treated samples were centrifuged at 10000 g for 5 min, washed twice with distilled water and then resuspended in 100 µL of distilled water. An aliquot (10 µL) of this suspension was spotted on a microscope slide, mounted with glass cover slip (diameter = 0.1-0.17 mm) (Fisher Scientific, UK) and observed with a fluorescent microscope (Leica DM IRB, Germany) using ×63 objective lens under oil immersion. TMR dextran particles (3 and 70 kDa) and 10 kDa Alexa 488 were excited using the green (530-550 nm) and blue (460-490 nm) excitation filter blocks, respectively. Ten images from different fields of view were captured under phase contrast and fluorescent views, and subsequently analysed. The percentage of fluorescent cells after separate exposures to E, H and E+H fields were calculated as the ratio of the total number of cell under phase contrast to the number of fluorescent cells. Cell suspensions containing fluorescent dextran particles without MW treatment was used as controls. All experiments were performed in triplicate and the percentage of fluorescent and non-fluorescent cells calculated as mean ± standard deviation (SD). To determine if MW exposure caused permanent damage to the cell wall, permeability to 10 kDa fluorescent dextran particles was assessed in *M. smegmatis* at 5, 10, 60, 120 and 300 seconds following MW E field exposure.

Theoretical and experimental calculation of bulk sample heating

To predict the rate of bulk heat generation following MW exposure of cell suspensions under the conditions used in this study, we employed a formula based on the definition of the specific heat capacity of the cell suspension, close to that of water C_w, of approximate value of 4.2 J/g/K. The initial rate of temperature rise in a sample during MW exposure is then defined as: $dT/dt = P/mC_w$, where m is the mass of the sample and P is the MW rms power dissipated. The total sample volume is 170 µL (i.e. a mass of approximately 0.17 g). Since the MW cavity is critically coupled and also, since the water sample provides the main load, the rms MW power dissipated is approximately the rms input power (P_{in}) generated by the MW circuitry, i.e. 12 W, which is reduced to an effective value of 0.12 W when taking into account the standard 1 % duty cycle. This yields an initial heating rate of approximately 0.17 ^{0}C/s over the standard 60 s exposure time, even if this initial heating rate were to be maintained the maximum possible temperature rise would be only 10 ^{0}C; in practice, heat transfer to the surroundings will limit this temperature rise to only a fraction of this maximum value, so we expect a temperature rise of a few ^{0}C at most. To validate this calculation, the temperature of samples during MW excitation was measured using a Luxtron fibre optic temperature sensor (LumaSense Technologies, Santa Clara, CA, USA). Using this temperature sensor probe, the bulk temperature increase of the cell suspension placed at the E field position was measured to be 2.6 ± 0.4 ºC over 60 seconds exposure time at 1 % duty cycle with 12 W rms power input (Fig 3) and this is entirely consistent with the calculation above.

Q factor measurement

The electric field at each of the E, E+H and H sample positions in the cavity was calculated using the following procedure. A 170µl sample within an Eppendorf tube was placed in the axial E position and the sample was critically coupled, such that $|S_{11}|$ at resonance was less

than −30dB. Whilst keeping the cavity coupling critically fixed for the E position, the sample was then (i) removed completely, (ii) placed back in the E position, (iii) placed in the E+H position and finally (iv) placed in the H position. In each case, values of the unloaded quality factor, resonant frequency and return loss (i.e. $IR = -20\,log|S_{11}|$ at resonance) were measured and the power absorbed by the sample was calculated, based on an input power of 12.0W.

Statistical Analysis

Results were analysed with SPSS (v.23). Significant differences within groups were determined using one-way analysis of variance (ANOVA) followed by a multiple comparison analysis using Tukey and Bonferroni tests.

Results

Cell membranes of micro-organisms act as a permeability barrier, protecting cells from the hostile environment and sustaining viability. Any breach in membrane permeability will increase the passage of chemicals in and out of the cell and will adversely affect viability.

Effect of MW on cell viability and the release of DNA

Cell viability (CFU/mL) was determined immediately after exposure to the MW E, H, and E+H fields and expressed as a percentage. Exposure to E, H and E+H field of MW radiation at the level used in this study had no significant effect (p>0.05) on the viability of any of the test microorganisms used in this study (Fig. 4). To determine if exposure to the same levels of MW radiation resulted in the release of DNA, we determined the concentration of DNA in cultures of *M. smegmatis* at pre- and post-exposure to E, H and E+H radiation. While we failed to detect the presence of increased concentration of DNA following exposure to E+H and H field exposure, we did see a significant increase (p<0.05) in DNA concentration following E field

exposure (Fig. 5). A possible reason for this difference is the fact that half of the E field energy is dissipated in the E+H field position as shown in our calculations.

MW E field induces PI internalisation

PI penetrates membrane injured cells, intercalates with nucleic acids and fluoresces red upon excitation, while cells with their membranes intact are impermeable to PI and do not stain red upon excitation. Permeability of membrane to PI was used to assess membrane integrity after *M. smegmatis* was treated with MW E fields. To compare with the effect of conventional heating, *M. smegmatis* cells were heated in a water bath to 37 °C. PI fluorescence significantly increased (p=0.0067) in MW treated cells but remained unchanged in heat-treated cells compared to controls (Fig. 6).

MW E-field induces dextran internalisation in cells in a size dependent manner

Fluorescent dextran particles have been used to determine membrane integrity (20). Thus, infiltration of dextran particles into MW exposed cells would suggest cell wall disruption. To determine if this was the case, cells were exposed to MW E, H and E+H fields in the presence of 3 kDa fluorescent dextran particles. While exposure to the H field and a combination of E+H fields had no effect on internalisation of 3 kDa dextran particles, all micro-organisms exposed to the E field alone exhibited a significant uptake of 3 kDa fluorescent dextran particles (p<0.05) (Fig. 7). To determine if the cell wall composition of a micro-organism affected its ability to internalise dextran particles following exposure to E field radiation, the relative ability of the cells to internalise 3 kDa dextran particles was compared (Fig. 8). Cells of *M. smegmatis* (50.4 ± 2.5%) demonstrated a significantly higher (p<0.05) level of particle uptake compared to the other isolates. The fluorescence of *C. albicans* (30.5 ± 2.1%) was significantly higher than those of *E. coli* (17.5 ± 1.9%) (p=0.01) but not in *S. aureus* (23.6 ± 4.6%) (p=0.096).

The variation in the degree of MW-mediated disruption in the organisms tested was determined by assessing their ability to internalise 10 and 70 kDa fluorescent dextran particles. All micro-organisms except for *S. aureus* internalised 10 kDa dextran particles while none of the organisms appeared to internalise 70 kDa dextran particles (Fig. S1). The low proportion of untreated cell populations that appeared fluorescent are likely to represent dead cells present in the cultures, or as the result of the centrifugation procedure employed, which may have induced membrane damage (28,29). Finally, the time taken for cells of *M. smegmatis* to regain membrane integrity and act as a permeability barrier after MW exposure was determined. Varying time intervals for adding dextran particles (10 kDa size) to bacterial suspension post verses pre-MW exposure was determined. The shortest time period to be investigated was 5 seconds, after which there was a 75.6% reduction in bacterial fluorescence (p<0.05). The percentage of fluorescent bacteria further reduced when dextran addition was delayed for 300 seconds (Fig. 9).

Determining MW power absorbed and Q factor at E, E+H and H positions

If the microwave input power is P_{in}, the microwave power absorbed by the cavity and its sample is $P_0 = \left(1-|S_{11}|^2\right)P_{\text{in}}$, where S_{11} is the voltage reflection coefficient at resonance. The power absorbed by the sample can then be calculated from

$$P_{\text{s}} = \left(1-\frac{Q_{\text{s}}}{Q_0}\right)P_0 = \left(1-\frac{Q_{\text{s}}}{Q_0}\right)\left(1-|S_{11}|^2\right)P_{\text{in}} \qquad (1)$$

where Q_{s} is the loaded quality factor of the cavity with the sample present and Q_0 is the unloaded quality factor of the empty cavity. The Q values when cavity is loaded separately with sample at the E, E+H and H field positions are presented in Table I below. The mean

electric field amplitude $\langle E_0 \rangle$ within the sample is calculated on the basis that the power absorbed by the sample can be written

$$P_s = \pi f_0 \varepsilon_2 \varepsilon_0 \langle E_0 \rangle^2 V_s \qquad (2)$$

where f_0 is the resonant frequency, ε_2 is the loss factor of the sample (assumed to be around 10 for an aqueous sample at a nominal frequency of 2.45GHz), $\varepsilon_0 = 8.85 \times 10^{-12}\,\mathrm{F/m}$ is the permittivity of free space and V_s is the sample volume (170μl). Simple inversion of Eqn (2) leads to

$$\langle E_0 \rangle = \sqrt{\frac{P_s}{\pi f_0 \varepsilon_2 \varepsilon_0 V_s}} \qquad (3)$$

from which $\langle E_0 \rangle$ is calculated, having first found P_s from Eqn.(1). Although $\langle E_0 \rangle$ does not account for electric field non-uniformity within the sample owing to the shape of the Eppendorf tube, it is a useful metric for comparing the microwave activity between the three sample positions. To estimate the magnitude of the microwave magnetic field $\langle H_0 \rangle$ around the perimeter of the cavity, for H field exposure with the sample at position C, we use the fundamental definition of quality factor to obtain

$$\langle H_0 \rangle \approx \sqrt{\frac{Q_0 P_0}{\pi \mu_0 f_0 V_c}}$$

where $\mu_0 = 4\pi \times 10^{-7}\,\mathrm{H/m}$ is the permeability of free space, $V_c = 266\,\mathrm{cm}^3$ is the cavity volume, $Q_0 = 2960 \pm 110$ is the unloaded quality factor of the empty cavity and $P_0 \approx 4.8\,\mathrm{W}$ is the part of the 12W incident power that is absorbed; P = 12W is the rms input power; these values yield $\langle H_0 \rangle = 70 \pm 2\,\mathrm{A/m}$.

Discussion

The biological effects of MWs are associated with thermal and non-thermal mechanisms. The former is attributed to temperature change while the latter is temperature independent and is thought to be due to the action of E and/ or H field effects (30). The present study focused on characterising the effect of each field, using a purpose-built TM_{010} mode resonant cavity, on the viability and permeability of structurally diverse micro-organisms. The cavity is designed so that the sample can be easily inserted and removed via a sample hole along its axis. Samples are contained in 300 µl Eppendorf tubes, typically containing 170 µl of sample. The MW field amplitudes are a function of the applied MW power and the sample volume. High control of these variables allows the field strengths to be calculated to an error of only ±2%, determined mostly by the uncertainty in sample volume. Our study showed the absence of synergy between E and H fields in inducing membrane disruption in the cells tested, contrary to what has been reported elsewhere (8). The result of this study cannot be compared to that of Novickij and colleagues as the MW parameters and treatment conditions are not comparable. Based on the design of our TM_{010} cavity, maximal E field energy is delivered at position A, halved at position B and is totally diminished at position C. Conversely, the magnitude of the H field is maximal, halved and diminished at positions C, B and A respectively.

The process of transforming cells is a frequent bacterial engineering technique. This may require chemical or electrical approaches. The latter is often referred to as electroporation. A major disadvantage of electroporation is the detrimental effect it has on cells viability (31). The magnitude of the E field applied to the cells in this study was lower than that used in classical electroporation (16), which probably explains why a significant reduction in cells viability was not observed. Additionally, MW pulsing (length and duration) are key parameters to induce

membrane permeabilization (32) and reduce viability. We believe that a combination of low MW power and the MW pulse conditions contributed to the cells' viability. While the viability of the micro-organisms was not affected, it did alter cell permeability to PI and different sized dextran particles. PI was permeable to cells of *M. smegmatis* after MW treatment but not in heat treated cells, suggesting that a specific MW E field dependent cell membrane disruption did occur. We sought to determine the extent to which cell membranes were disrupted by determining their uptake to varying size of dextran particles. Cells of *M. smegmatis* were the most sensitive and *S. aureus* the least. These results are likely to reflect differences in cell wall and membrane composition (19,21). The mechanisms by which the E field interacts with biological cells remains unclear. High frequency vibration of cell membranes (mechanical cell stimulation), enhanced diffusion across membranes, abnormal gating of voltage channels, increased membrane conductance and pore formation have been cited as possible mechanisms (9,10,33–39). Pore formation has been likened to electroporation (20,40–42). Although this is frequently reported, no experimental data have captured pores in cell membranes following MW exposure except in computer simulations studies.

In electroporation, a constant (i.e. DC) E field of magnitude usually between 10 to 100 kV/m when applied to cells induces temporary membrane pores which allows the delivery of exogenous substance (e.g. DNA, drugs) into cells and endogenous substances to be extracted (13,35,41,43–45). The process begins by the interaction of water molecules with membrane phospholipids as a consequence of the application of E field energy (46,47). This interaction induces membrane deformity characterised by reorientation of lipid molecules at the water membrane interface. The result is the formation of a pores usually between 0.5 to 400 nm in size (38,41,42). The time taken to reform the membrane depends on the magnitude of the E field, nature of the membrane, and can range from seconds to 10 mins (21).

Biological membranes act as electrical insulators and have the ability to maintain cells ionic balance. For influx/efflux mechanism to occur, the membrane must be destabilised, and this can be achieved via thermal or external influence e.g. electrically. The membrane potential of any cell ranges between +30 mV in mammalian cells to -300 mV in plant cells to maintain its ionic balance (48). The application of an external E field higher than the membrane potential causes membrane instability and compromises barrier functionality. Since membrane permeabilization was observed only after E field excitation, we reason that the stability of cell membrane macromolecules (e.g. proteins, lipids) may have been weakened, transitioning them from their stable impermeable state to a permeable one. As a result of this perturbation, membranes may have become leaky, thus facilitating efflux and influx phenomena.

We also attempted to minimize localised heating effects by restricting the bulk temperature rise. While we were able to minimise the temperature rise to 2.6°C, this is unlikely to be a true reflection of the temperature at the cell membrane surface. Thus, the effects observed may still reflect a combination of thermal and non-thermal effects. Further work is required to distinguish the contribution of these two forms of energy (i.e. thermal and electric). The rapid release of DNA from cells following MW treatment is also an improvement on the current DNA extraction methodologies. The released DNA may be employed for downstream applications (e.g. PCR, DNA hybridisation) and to support the development of point-of-care applicators.

Conclusion

We have shown that MW generated E fields can temporarily disrupt membrane integrity resulting in the uptake of dextran particles and the release of DNA. By optimising this

approach, it may be possible to transform cells with foreign particles (e.g. DNA) and minimizing cell damage. Further studies are required to determine if this is indeed the case.

Supplementary Material

Fluorescent images of cells showing uptake of mostly 3kDa and 10 kDa but not 70 kDa dextran particles following MW treatment.

Figure 1. Schematic diagram of the bench-top microwave application system.

Figure 2. (Left) COMSOL simulation results showing E and H field distribution inside the cavity. (Right) An illustration showing all sample tube positions (A, B, and C) inside the cavity aligned with normalized E field maximum (A), mixed E+H field (B), and near H-field maximum (C), respectively. In the experiment only one tube was inserted at a time. The distances between A-B and A-C are 27 mm and 42 mm, respectively.

Figure 3. Measured and theoretical temperature measurement in sample tube following microwave excitation. A total volume of 170 μL water was excited with MW energy (at 0.1%, 1% and 10% duty cycle) for the 10 seconds. Temperature change was measured with the temperature probe sensor. The MW setup values align with the values align with those predicted theoretically. Error bars indicate the standard deviation of results (n=3).

Figure 4. The effects of E, H and E+H fields on cell viability. Cell viability after exposure to E, H and E+H fields was determined and expressed as percentage. Viability reduced (but not significantly) in cells treated with E fields alone (p>0.05), while cells treated with H and E+H fields remained unaffected as untreated. Data are mean ± SD of three independent experiments.

Figure 5. Release of double stranded DNA (dsDNA) after MW exposure. A suspension of *M. smegmatis* was treated with MW E, H and E+H fields at 1% duty cycle for 60 secs. The concentration of dsDNA released was significant ($p<0.05$) in suspensions treated with MW E field alone. Data are mean ± SD of three independent experiments.

Figure 6. Quantification of PI fluorescence in *M. smegmatis* after MW treatment. PI stained cells were treated with one of each MW E, E+H and H fields, and conventional heating at 37 °C. Membrane permeability was significantly increased ($p = 0.0067$) following MW E field treatment. Cells subjected to thermal treatment at 37 °C did not increase membrane permeability to PI and was similar to the control (untreated). Control represents PI stained cells without any treatment. Data represent mean ± SD of three independent experiments.

Figure 7. Quantification of fluorescent cells after separate exposure to MW E, H and E+H fields. Cells exposed to E+H-field (grey bars) and H-field (white bars) did not result in significant uptake of 3 kDa dextran particle in all cells tested as compared to the control group (orange bar) ($p>0.05$). Cells exposed to E field alone (dark bars) resulted in a significant uptake of 3 kDa fluorescent dextran particle ($p<0.05$). Values represent mean ± SD of three independent experiments.

Figure 8. Quantification of fluorescent cells after MW E-field exposure. The percentage of fluorescent cells after MW treatment (grey bars) and the corresponding untreated cells (white bars) was determined for each dextran particle size. Percentage of fluorescent cells was calculated as a ratio of the number of cells in fluorescent view to the total number counted under phase contrast. The percentage of fluorescent cells with 3 kDa dextran uptake was

significantly high in *M. smegmatis* than in all cells (p<0.05) and in *C. albicans* in comparison to *E. coli* (p=0.01). Fluorescent cells of *M. smegmatis* and *S. aureus* decreased significantly when dextran size was increased to 10 kDa (p<0.05). None of the cells internalised the 70 kDa dextran particle. The labels (*) and (***) corresponds to (p<0.05) and (p<0.001) respectively and are statistically significant between the groups compared. Values represent mean ± SD of three independent experiments.

Figure 9. Time taken to regain membrane integrity following MW exposure**.** Addition of dextran particles (10 kDa) to MW E field treated bacterial suspension was delayed for 5s, 10s, 1 min and 5 min. The percentage of fluorescent bacteria was significantly high (p<0.05) in MW treated suspensions containing dextran particle (t=0) than when the addition of dextran particle was delayed and in untreated. Values represent mean ± SD of two independent experiments.

Fig S1. Uptake of varying sizes of fluorescent dextran particles into cells after MW E-field exposure. The images have been captured under phase contrast and fluorescent fields following 3 kDa, 10 kDa and 70 kDa dextran application to MW treated cell suspensions of *M. smegmatis* (NCTC 8159), *E. coli* (NCTC 1093), *C. albicans* (NCPF 3179) and *S. aureus* (NCTC 13373) with corresponding controls (MW untreated). Images in phase contrast are of the same field as fluorescent view. Mostly 3 kDa and 10 kDa dextrans were internalised in *M. smegmatis*, *E. coli*, *C. albicans* but not 70 kDa. Only 3 kDa was internalised in *S. aureus*. Scale bars correspond to 20µm.

Table I: microwave exposure parameters for samples in the three different positions.

Position	$f_0\,(\mathrm{GHz})$	$IL\,(\mathrm{dB})$	Q_s	$P_\mathrm{s}\,(\mathrm{W})$	$\langle E_0 \rangle\,(\mathrm{kV/m})$
E	2.433 ± 0.001	-39.4 ± 2.5	494 ± 7	11.8 ± 0.2	9.3 ± 0.1
E+H	2.478 ± 0.001	-6.84 ± 0.05	1080 ± 20	6.5 ± 0.2	6.6 ± 0.1
H	2.501 ± 0.001	-2.19 ± 0.01	2720 ± 70	0.4 ± 0.2	1.6 ± 0.4

The empty resonator has $f_0 = 2.502 \pm 0.001\,\mathrm{GHz}$, $IL = -39.7 \pm 2.5\,\mathrm{dB}$, $Q_0 = 2960 \pm 110$

Author contribution

EKA, LB and AP conceived the experiment. EKA performed the experiment, analysed the results and prepared the manuscript. LB and AP supervised the work and revised the manuscript. DM, CFW and JL provided guidance to the experiment and revised the manuscript. HC modelled microwave fields in COMSOL. All authors reviewed the manuscript.

Acknowledgement

Dr Heungjae Choi holds Sêr Cymru II Fellowship part-funded by the European Regional Development Fund through the Welsh government (TG/KJB/VSM:1103515).

Additional Information

We have no conflict of interest to declare

Data Availability

The data that supports the findings of this study are available within the article [and its supplementary material].

References

1. Zielinska M, Ropelewska E, Xiao H-W, Mujumdar AS, Law CL. Review of recent applications and research progress in hybrid and combined microwaveassisted drying of food products: Quality properties. Crit Rev Food Sci Nutr. 2019;1–53.

2. Rosen A, Stuchly MA, Vorst AV. Applications of RF/microwaves in medicine. EEE Trans Microw Theory Tech. 2002;50(3):963–74.

3. Dawkins AWJ., Nightingale NRV., South GP, Sheppard RJ, Grant EH. The role of water in microwave absorption by biological material with particular reference to microwave hazards. Phys Med Biol. 1979;24(6):1168–76.

4. Antonio C, Deam R. Can '"microwave effects"' be explained by enhanced diffusion? Phys Chem Chem Phys. 2007;9:2976–82.

5. Banik S, Bandyopadhyay S, Ganguly S. Bioeffects of microwave - a brief review. Bioresour Technol. 2003;87(2):155–159.

6. Asay B, Zinaida T, Anastasia V, Maggie W. Membrane composition as a factor in susceptibility of Escherichia coli C29 to thermal and non-thermal microwave radiation. J Exp Microbiol Immunol. 2008;12:7–13.

7. Kardos TJ, Rabussay DP. Contactless magneto-permeabilization for intracellular plasmid DNA delivery in-vivo. Hum Vaccin Immunother. 2012;8(11):1707–13.

8. Novickij V, Grainys A, Lastauskienė E, Kananavičiūtė R, Pamedytytė D, Kalėdienė L, et al. Pulsed electromagnetic field assisted in vitro electroporation: A pilot study. Sci Rep. 2016;6:33537.

9. Pall ML. Electromagnetic fields act via activation of voltage-gated calcium channels to produce beneficial or adverse effects. J Cell Mol Med. 2013;17(8):958–65.

10. Pall ML. Scientific evidence contradicts findings and assumptions of Canadian Safety Panel 6: microwaves act through voltage-gated calcium channel activation to induce biological impacts at non-thermal levels, supporting a paradigm shift for microwave/lower freque. Rev Env Heal. 2015;30(2):99–116.

11. Bu B, Tian Z, Li D, Ji B. High transmembrane voltage raised by close contact initiates fusion pore. Front Mol Neurosci. 2016;9:136.

12. Levine ZA, Vernier PT. Life cycle of an electropore: field-dependent and field-independent steps in pore creation and annihilation. J Membr Biol. 2010;236(1):27–36.

13. Ramos C, Bonato D, Winterhalter M, Stegmann T, Teissie J. Spontaneous lipid vesicle fusion with electropermeabilized cells. FEBS Lett 2002 518 p. 2002;518:135–8.

14. Weaver JC, Chizmadzhev YA. Theory of electroporation: A review. Bioelectrochemistry Bioenerg. 1996;41(2):135–60.

15. Gehl J. Electroporation: theory and methods, perspectives for drug delivery, gene therapy and research. Acta Physiol Scand. 2003;177(4):437–47.

16. Chassy BM, Mercenier A, Flickinger J. Transformation of bacteria by electroporation. Trends in Biotech. 1988;6(12):303–9.

17. Elder JA, Cahill DF. Biological effects of radiofrequency radiation. US Environ. 1984. 259 p.

18. Rougier C, Prorot A, Chazal P, Leveque P, Lepratb P. Thermal and nonthermal effects of discontinuous microwave exposure (2.45 Gigahertz) on the cell membrane of Escherichia coli. Appl Env Microbiol. 2014;80(16):4832–4841.

19. Nguyen THP, Pham VTH, Nguyen SH, Baulin V, Croft RJ, Phillips B, et al. The Bioeffects Resulting from Prokaryotic Cells and Yeast Being Exposed to an 18 GHz Electromagnetic Field.

PLoS One. 2016;11(7):e0158135.

20. Shamis Y, Taube A, Mitik-Dineva N, Croft R, Crawford RJ, Ivanova EP. Specific electromagnetic effects of microwave radiation on Escherichia coli. Appl Env Microbiol. 2011;77(9):3017–22.

21. Nguyen TH, Shamis Y, Croft RJ, Wood A, McIntosh RL, Crawford RJ, et al. 18 GHz electromagnetic field induces permeability of Gram-positive cocci. Sci Rep 16;510980 doi. 2015;5:10980.

22. Waldron RA. Perturbation theory of resonant cavities. Proc Inst Elec Eng. 1960;107C:272–4.

23. Pozar DM. Microwave engineering. 4th ed. New York, NY: Wiley; 2011.

24. Mehdizadeh M. Microwave/RF Applicators and Probes for Material Heating, Sensing, and Plasma Generation. Second edi. William Andrew Publishing; 2015. 109–150 p.

25. Cunliffe A, Mathias LES. Some perturbation effects in cavity resonators. Proc IEE-Part III Radio Commun Eng. 1950;97:367–76.

26. Chatterjee SK. Microwave cavity resonators. some perturbation effects and their appli cations. Radio Eng J Br Inst. 1953;13:475–84.

27. Miles AA, Misra SS, Irwin JO. The estimation of the bactericidal power of the blood. J Hyg. 1938;38(6):732–749.

28. Shi L, Günther S, Hübschmann T, Wick LY, Harms H, Müller S. Limits of propidium iodide as a cell viability indicator for environmental bacteria. Cytom A. 2007;71(8):592–8.

29. Peterson BW, Sharma PK, van der Mei HC, Busscher HJ. Bacterial cell surface damage due to centrifugal compaction. Appl Env Microbiol. 2012;78(1):120–5.

30. Challis LJ. Mechanisms for interaction between RF fields and biological tissue. Bioelectromagnetics. 2005;26(S7):98–106.

31. Kang S, Kim KH, Kim YC. A novel electroporation system for efficient molecular delivery into Chlamydomonas reinhardtii with a 3-dimensional microelectrode. Sci Rep. 2015;5:15835.

32. Rols M. P, Teissié J. Electropermeabilization of mammalian cells to macromolecules: control by pulse duration. Biophys J. 1998;75(3):1415–1423.

33. Benz R, Zimmermann U. Pulse-length dependence of the electrical breakdown in lipid bilayer membranes. Biochim Biophys Acta. 1980;597(3):637–42.

34. Böckmann RA, de Groot BL, Kakorin S, Eberhard N, Helmut G. Kinetics, statistics, and energetics of lipid membrane electroporation studied by molecular dynamics simulations. Biophys J. 2008;95(4):1837–50.

35. Dower WJ, Miller JF, Ragsdale CW. High efficiency transformation of E.coli by high voltage electroporation. Nucleic Acids Res. 1988;16(13):6127–45.

36. Hibino M, Itoh H, Kinosita KJ. Time courses of cell electroporation as revealed by submicrosecond imaging of transmembrane potential. Biophys Joumal. 1993;64(6):1789–800.

37. Krassowska W, Filev PD. Modeling electroporation in a single cell. Biophys J. 2007;92(2):404–17.

38. Marrink JS, de Vriesa HA, Tieleman PD. Lipids on the move: Simulations of membrane pores, domains, stalks and curves. Biochim Biophys Acta - Biomembr. 2009;1788(1):149–68.

39. Pall ML. Electromagnetic field activation of voltage-gated calcium channels: role in

therapeutic effects. Electromagn Biol Med. 2014;33(4):251.

40. Kinosita KJ, Tsong TY. Voltage-Induced Pore Formation and Hemolysis of Human Erythrocytes. Biochim Biophys Acta. 1977;471(2):227–42.

41. Tieleman DP. The molecular basis of electroporation. BMC Biochem. 2004;5:10.

42. van Uitert I, Gac SL, van den Berg A. Determination of the electroporation onset of bilayer lipid membranes as a novel approach to establish ternary phase diagrams: example of the l-α-PC/SM/cholesterol system. Soft Matter. 2010;6(18):4420.

43. Chassy BM, Mercenier A, Flickinger J. Transformation of bacteria by electroporation. Trends Biotechnol. 1988;6(12):303–9.

44. Smith KC, Neu JC, Krassowska W. Model of Creation and Evolution of Stable Electropores for DNA Delivery. Biophys J. 2004;86(5):2813–2826.

45. Wang L, Liu D, Zhou R, Wang Z, Cuschieri A. Tumour cell membrane poration and ablation by pulsed low-intensity electric field with carbon nanotubes. Int J Mol Sci. 2015;16(4):6890–901.

46. Vernier PT, Ziegler MJ. Nanosecond Field Alignment of Head Group and Water Dipoles in Electroporating Phospholipid Bilayers. J Phys Chem B. 2007;111(45):12993–6.

47. Ziegler MJ, Vernier PT. Interface water dynamics and porating electric fields for phospholipid bilayers. J Phys Chem B. 2008;112(43):13588–13596.

48. Pliquett U, Schoenbach RP, Joshi V, Sridhara KH. High electrical field effects on cell membranes. Bioelectrochemistry. 2007;70(2):275–82.

Figures

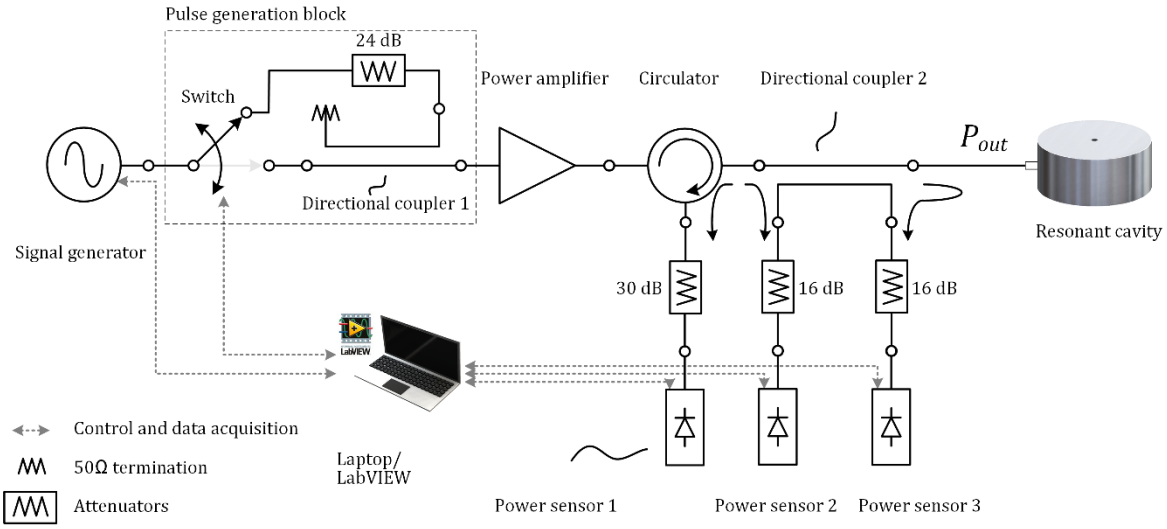

Figure 1. Schematic diagram of the bench-top microwave application system.

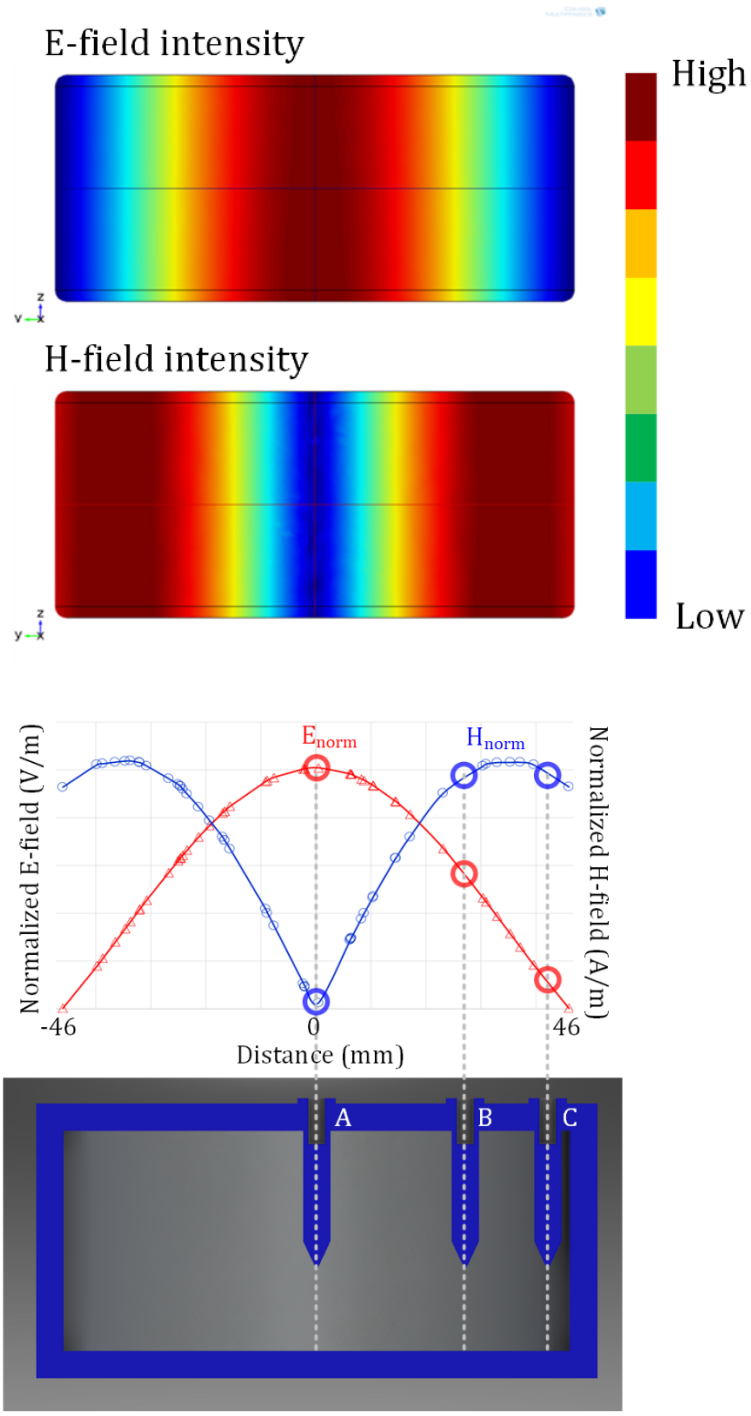

Figure 2. (Left) COMSOL simulation results showing E and H field distribution inside the cavity. (Right) An illustration showing all sample tube positions (A, B, and C) inside the cavity aligned with normalized E field maximum (A), mixed E+H field (B), and near H-field maximum (C), respectively. In the experiment only one tube was inserted at a time. The distances between A-B and A-C are 27 mm and 42 mm, respectively.

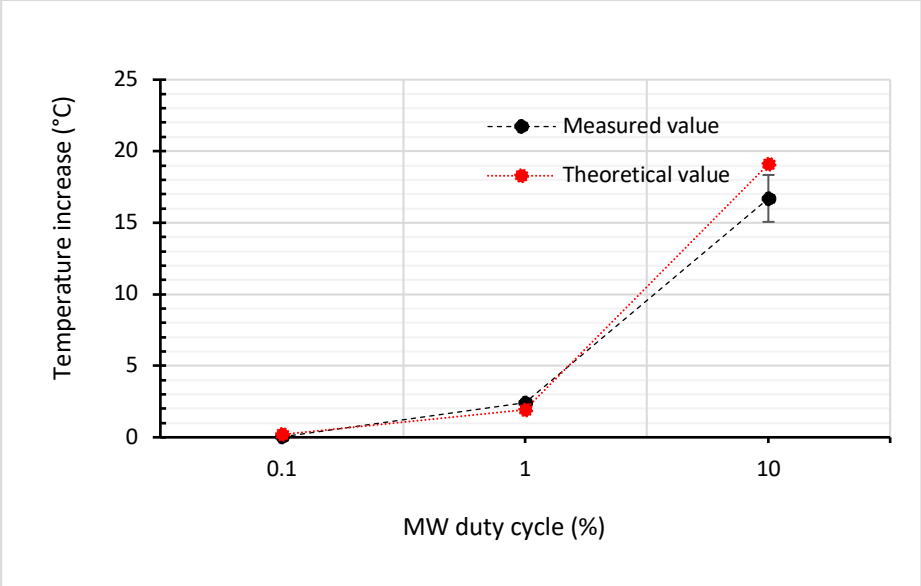

Figure 3. Measured and theoretical temperature measurement in sample tube following microwave excitation. A total volume of 170 µL water was excited with MW energy (at 0.1%, 1% and 10% duty cycle) for the 10 seconds. Temperature change was measured with the temperature probe sensor. The MW setup values align with the values align with those predicted theoretically. Error bars indicate the standard deviation of results (n=3).

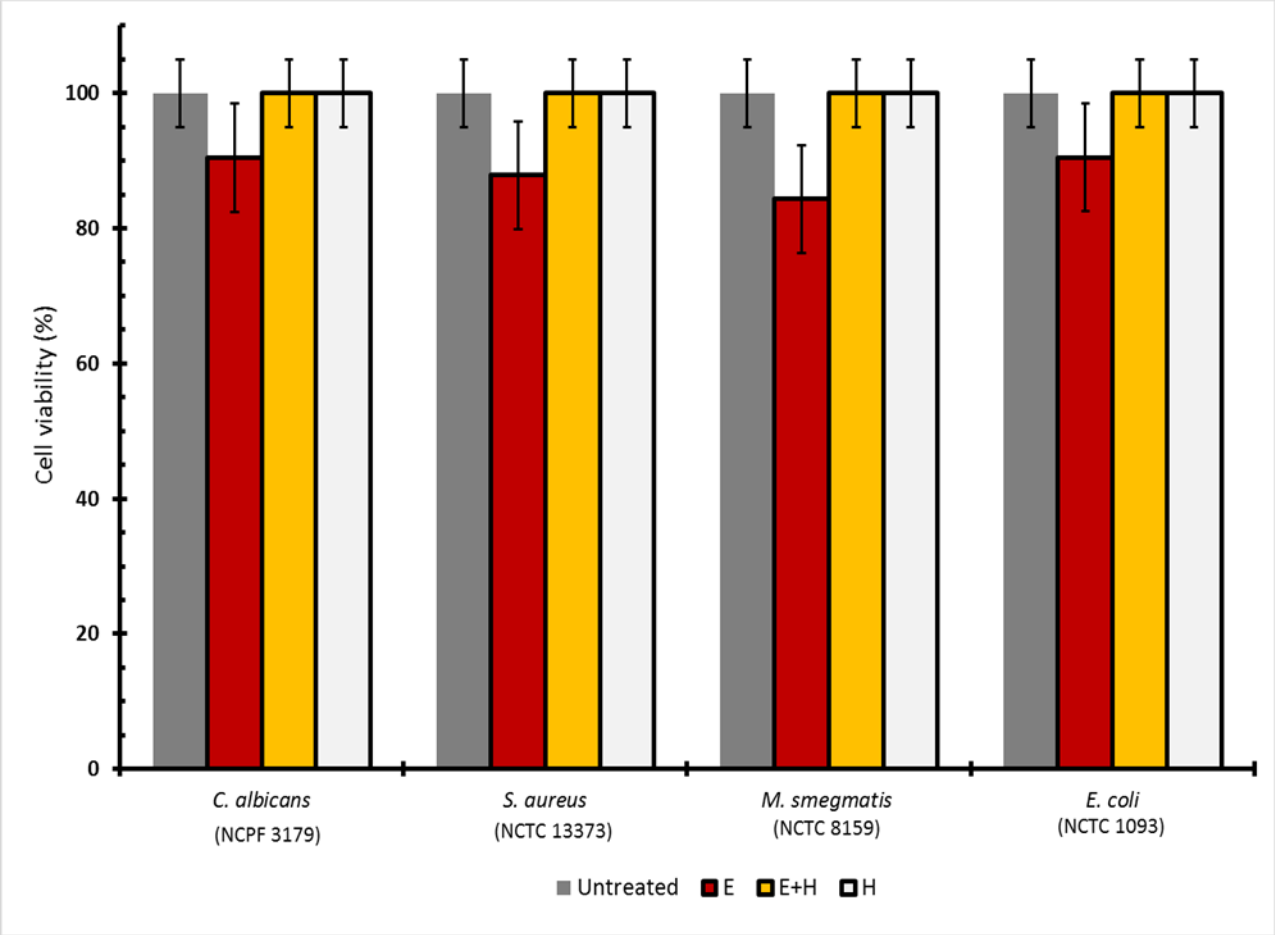

Figure 4. The effects of E, H and E+H fields on cell viability. Cell viability after exposure to E, H and E+H fields was determined and expressed as percentage. Viability reduced (but not significantly) in cells treated with E fields alone (p>0.05), while cells treated with H and E+H fields remained unaffected as untreated. Data are mean ± SD of three independent experiments.

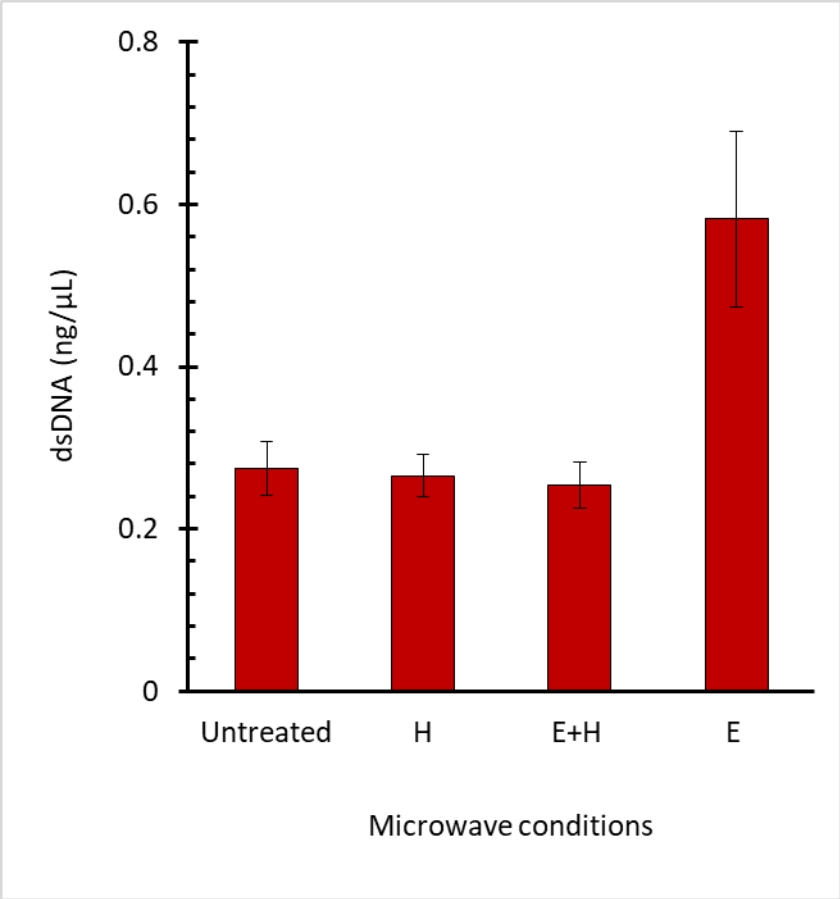

Figure 5. Release of double stranded DNA (dsDNA) after MW exposure. A suspension of *M. smegmatis* was treated with MW E, H and E+H fields at 1% duty cycle for 60 secs. The concentration of dsDNA released was significant ($p<0.05$) in suspensions treated with MW E field alone. Data are mean ± SD of three independent experiments.

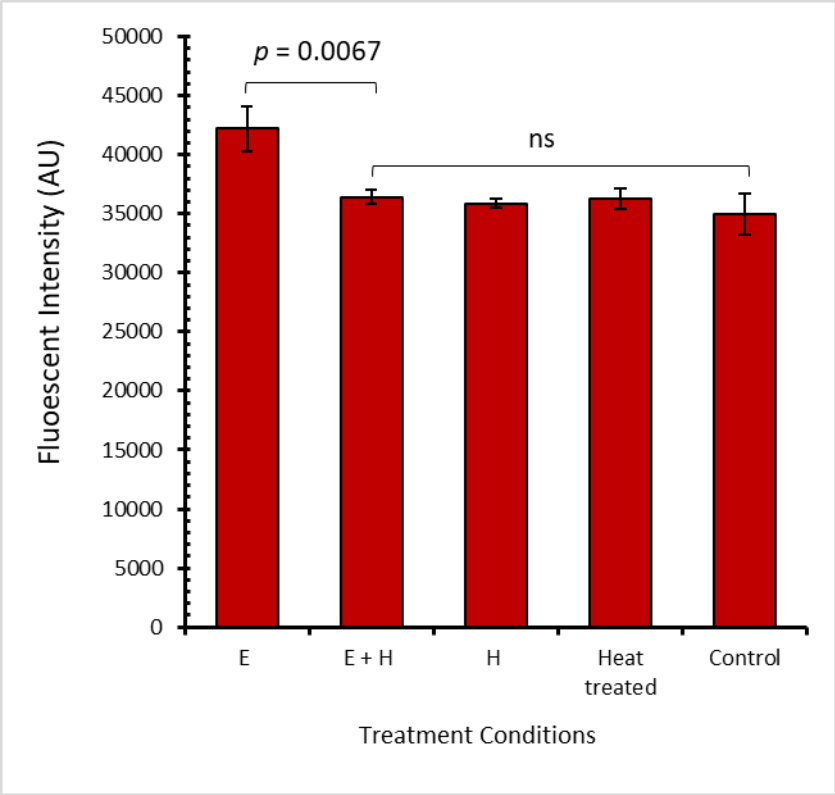

Figure 6. Quantification of PI fluorescence in *M. smegmatis* after MW treatment. PI stained cells were treated with one of each MW E, E+H and H fields, and conventional heating at 37 °C. Membrane permeability was significantly increased (p = 0.0067) following MW E field treatment. Cells subjected to thermal treatment at 37 °C did not increase membrane permeability to PI and was similar to the control (untreated). Control represents PI stained cells without any treatment. Data represent mean ± SD of three independent experiments.

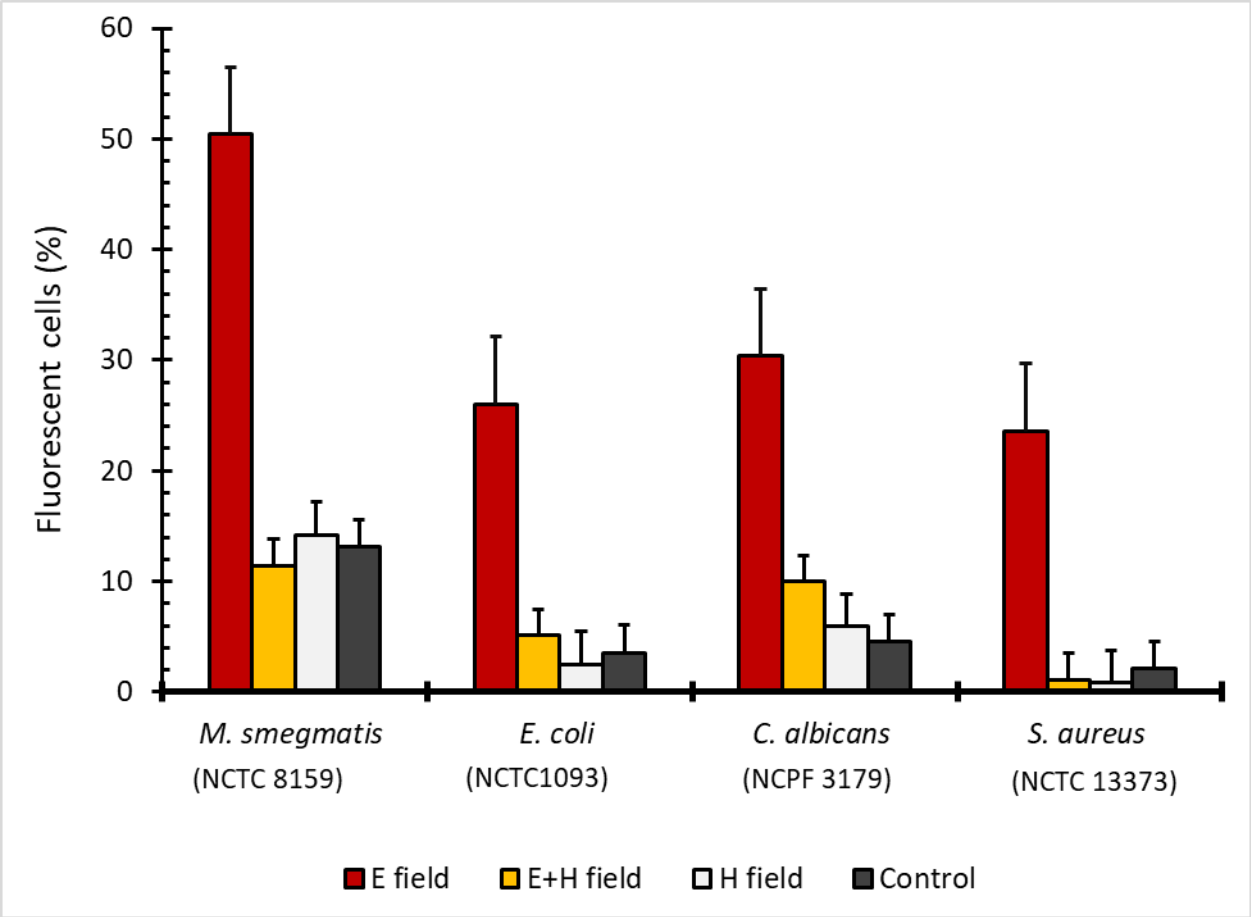

Figure 7. Quantification of fluorescent cells after separate exposure to MW E, H and E+H fields. Cells exposed to E+H-field (grey bars) and H-field (white bars) did not result in significant uptake of 3 kDa dextran particle in all cells tested as compared to the control group (orange bar) ($p>0.05$). Cells exposed to E field alone (dark bars) resulted in a significant uptake of 3 kDa fluorescent dextran particle ($p<0.05$). Values represent mean ± SD of three independent experiments.

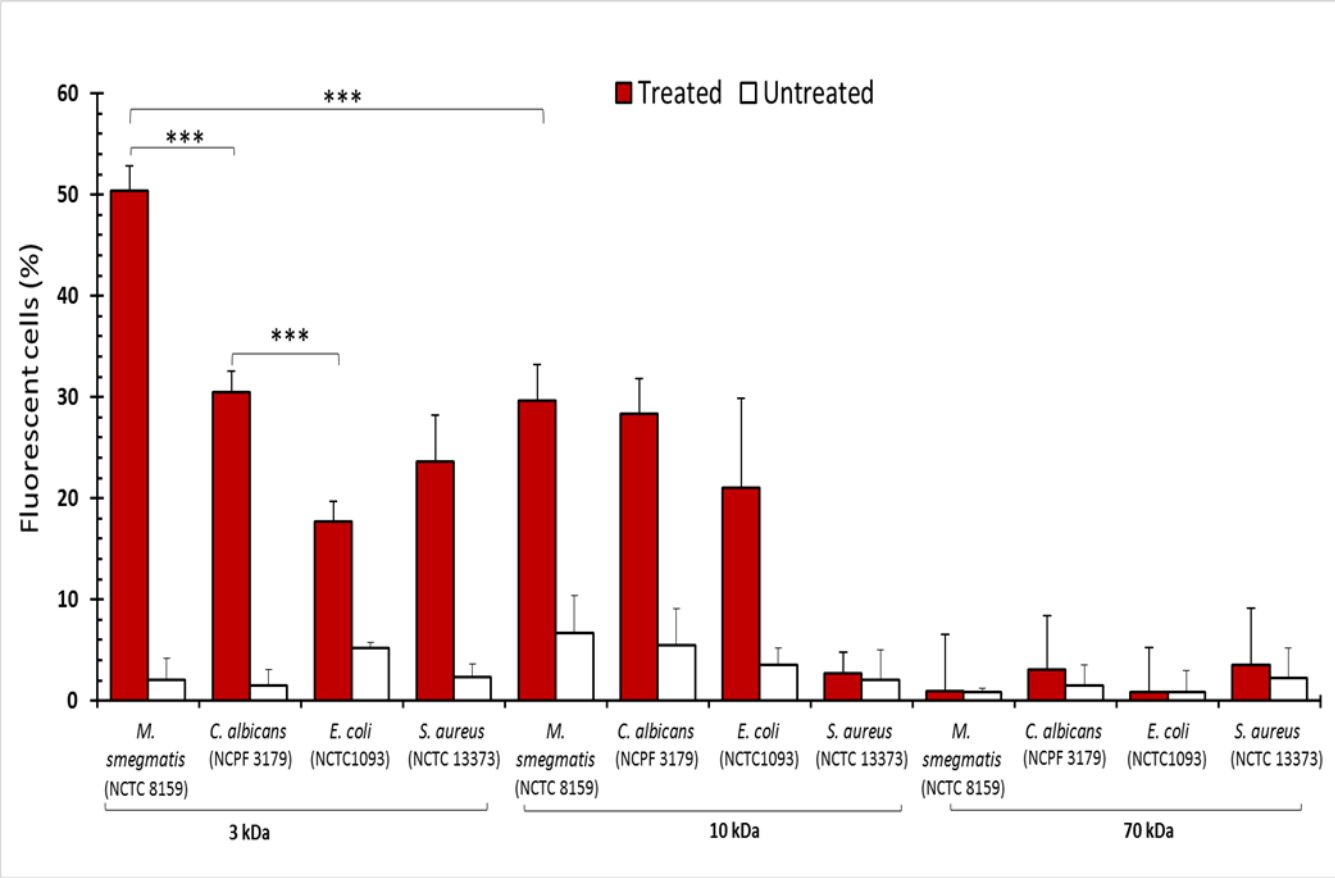

Figure 8. Quantification of fluorescent cells after MW E-field exposure. The percentage of fluorescent cells after MW treatment (grey bars) and the corresponding untreated cells (white bars) was determined for each dextran particle size. Percentage of fluorescent cells was calculated as a ratio of the number of cells in fluorescent view to the total number counted under phase contrast. The percentage of fluorescent cells with 3 kDa dextran uptake was significantly high in *M. smegmatis* than in all cells (p<0.05) and in *C. albicans* in comparison to *E. coli* (p=0.01). Fluorescent cells of *M. smegmatis* and *S. aureus* decreased significantly when dextran size was increased to 10 kDa (p<0.05). None of the cells internalised the 70 kDa dextran particle. The labels (*) and (***) corresponds to (p<0.05) and (p<0.001) respectively and are statistically significant between the groups compared. Values represent mean ± SD of three independent experiments.

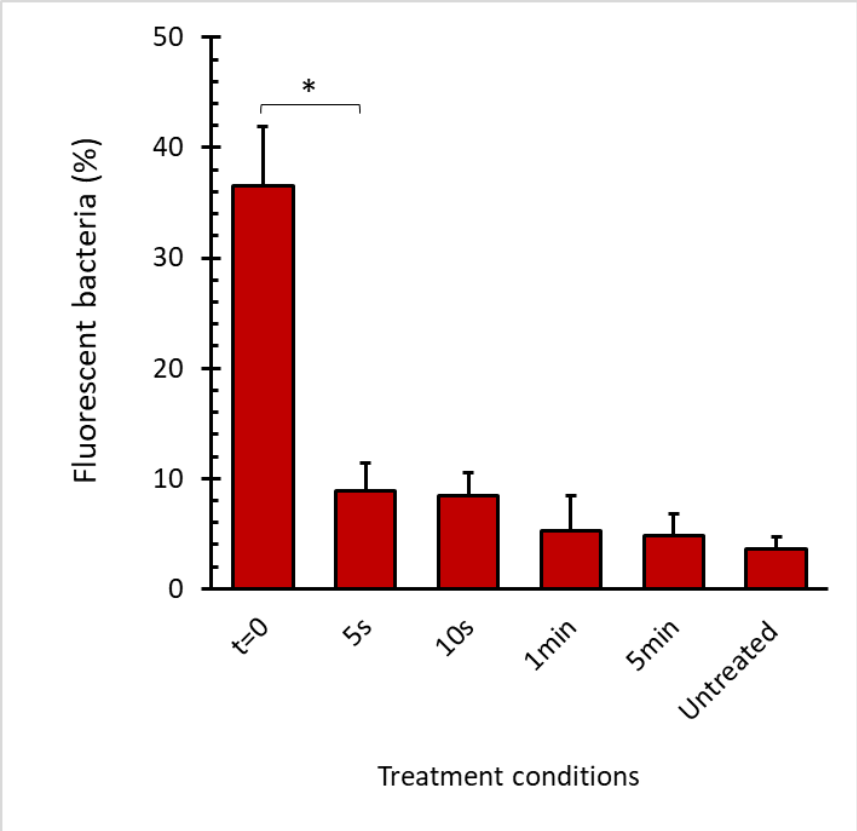

Figure 9. Time taken to regain membrane integrity following MW exposure**.** Addition of dextran particles (10 kDa) to MW E field treated bacterial suspension was delayed for 5s, 10s, 1 min and 5 min. The percentage of fluorescent bacteria was significantly high (p<0.05) in MW treated suspensions containing dextran particle (t=0) than when the addition of dextran particle was delayed and in untreated. Values represent mean ± SD of two independent experiments.

Supplementary material

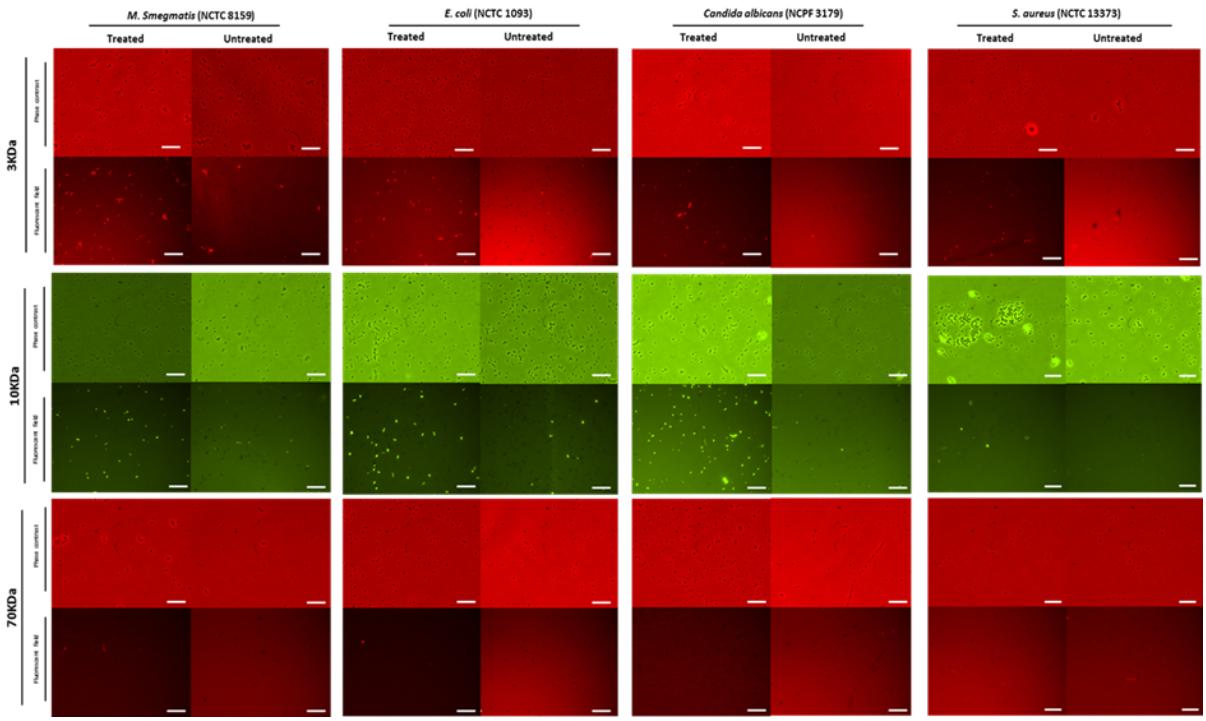

Fig S1. Uptake of varying sizes of fluorescent dextran particles into cells after MW E-field exposure. The images have been captured under phase contrast and fluorescent fields following 3 kDa, 10 kDa and 70 kDa dextran application to MW treated cell suspensions of *M. smegmatis* (NCTC 8159), *E. coli* (NCTC 1093), *C. albicans* (NCPF 3179) and *S. aureus* (NCTC 13373) with corresponding controls (MW untreated). Images in phase contrast are of the same field as fluorescent view. Mostly 3 kDa and 10 kDa dextrans were internalised in *M. smegmatis*, *E. coli*, *C. albicans* but not 70 kDa. Only 3 kDa was internalised in *S. aureus*. Scale bars correspond to 20µm.